

Microstructure and Micro-mechanical Properties of Cu Based Amorphous Composites with Shape-Memory Crystals

Yuan Xiaopeng^{1,2}, Zhao Yanchun^{1,2}, Kou Shengzhong^{1,2}, Zhao Zhiping^{1,2}, Li Chunyan^{1,2}, Yuan Zizhou^{1,2}

¹ State Key Laboratory of Advanced Processing and Recycling of Non-ferrous Metals, Lanzhou University of Technology, Lanzhou 730050, China; ² Wenzhou Research Institute of Pump and Valve Engineering of Lanzhou University of Technology, Wenzhou 325105, China

Abstract: Tapered $\text{Cu}_{50}\text{Zr}_{42}\text{Al}_8$ alloy with good glass-forming ability was fabricated by copper mould suction casting. Cubic AlCu_2Zr and B2-ZrCu, thermal-induced martensitic B19'-ZrCu phases form on the glass matrix along the radial direction structure. Size effects on micro-mechanical properties and a unique crack healing behavior were studied. Micro-hardness of monolithic bulk metallic glass (BMG) displays "smaller is softer" trend, that is, the softer surface and the harder center. Whereas the larger size composites possess a softer center and a harder surface, due to the integrative action of the secondary phases. Amorphous matrix is toughened by TRIP (transition induced plasticity) effect of shape-memory phase as well as weakened and embrittled by AlCu_2Zr crystal. After annealing, self-healing of Vickers indentation crack occurs as the thermoelastic transformation of shape-memory crystals. As loading, stress-induced martensites transform from B2 to B19', along with volume expansion. Annealed upon the reverse transformation temperature, B19' to B2 transform accompanied by a volume shrinkage, and a restoring force from the structure stress is set up to drive the crack closure.

Key words: bulk metallic glass composites; shape-memory crystals; micro-mechanical behavior; self-healing

Bulk metallic glass (BMG) is a new family of metallic alloys with thickness larger than 1 mm and formed at relatively low cooling rates in the range of 1~100 K/s^[1,2]. Amorphous atomic structure leads to a unique set of characteristic properties for the family of BMGs, such as superior strength and elastic limit, high corrosion-resistance, and good soft magnetism, which far exceed the properties currently available in crystalline metals^[3,4]. For example, a yield strength over 1722.5 N/mm² ksi has been achieved in Zr-based BMGs (Vit-001 series by Liquidmetal Technology), that is, more than 2.5 times the strength and more than 50 times the plasticity of conventional $\text{Ti}_6\text{Al}_4\text{V}$ alloy, which possess superplastic formability in the supercooled liquid region like the plastic^[5]. Since A. Inoue succeeded in finding new multicomponent alloy systems consisting mainly of

common metallic elements with lower critical cooling rates in the late 1980 s, scientists have done a lot to find new kinds of bulk metallic glasses and their composites with high glass forming ability (GFA) and excellent performances^[6-10]. Among them, CuZr based BMG alloys have been considered as the promising structural and functional materials because of their unique physical and mechanical properties, good processibility and low cost^[11,12]. In the present paper, microstructure, micro-mechanical behavior, and a unique crack healing behavior of $\text{Cu}_{50}\text{Zr}_{42}\text{Al}_8$ were investigated. And size effect on microstructure and micro-mechanical properties was discussed.

1 Experiment

Element pieces (purity > 99.9%) were used as starting materials. $\text{Cu}_{50}\text{Zr}_{42}\text{Al}_8$ (at%) ingots used as master alloys were

Received date: January 14, 2016

Foundation item: National Natural Science Foundation of China (51551101, 51661017, 51571105); Specialized Research Fund for the Doctoral Program of Higher Education (20116201120003); Natural Science Foundation of Zhejiang Province of China (LQ13E010002); Scientific Research Project of the Higher Education Institutions of Gansu Province (2013A-040)

Corresponding author: Zhao Yanchun, Ph. D., Associate Professor, State Key Laboratory of Gansu Advanced Non-ferrous Metal Materials, Lanzhou University of Technology, Lanzhou 730050, P. R. China, E-mail: yanchun_zhao@163.com

Copyright © 2017, Northwest Institute for Nonferrous Metal Research. Published by Elsevier BV. All rights reserved.

prepared by copper mold casting under a Ti-gettered argon atmosphere. To ensure the homogenization of the elements in the ingots, the master alloys were melted for three times. Then the master alloys were re-melted in quartz tubes in a purified inert atmosphere by a suction casting furnace, and injected into a water-cooled copper mould with a tapered cavity of 80 mm in length and 10 mm in bottom diameter. The microstructure of samples etched with 10 wt% HNO_3 after carefully mechanical polishing was observed by optical microscope. Phase were determined by X-ray Diffraction (XRD) using $\text{Cu K}\alpha$ radiation (40 kV, 30 mA). The microstructure was identified by transmission electron microscope (TEM, Phillips CM20) with an accelerating voltage 200 kV. TEM sample was prepared with ion milling process. The cylindrical samples were cut into cylinders and the surfaces were ground flat to parallel before the hardness test. The Vickers hardness was measured by a MH-5 Vickers micro-hardness tester with a load of 200 g holding for 15s. Specimens for nanoindentation tests were prepared similarly for the microhardness test but were polished to a mirror like finish before the test. Depth-sensing indentation was conducted with a Nanotest 600 instrument (Micro Materials Ltd, UK) fitted with a Berkovich indenter. Penetration depth was 400 nm and the load-displacement curves, including unloading, were analyzed to extract values of hardness and plastic deformation.

2 Results and Discussion

2.1 Microstructure of Cu based amorphous composite

Fig.1 is XRD patterns of tapered sample with different diameters. We can see, the samples of diameter 4.0, 4.4 and 4.8 mm show a unitary amorphous phase as only a broad diffuse peak between the diffraction angles 30° and 50° displays. Samples with larger sizes start to be crystallized. Some crystals in samples of diameter 4.9 and 5.0 mm, are identified as AlCu_2Zr (CsCl Structure, Pearson Symbol cP2 Space Group Pm $\bar{3}$ m, $a=0.311$ nm), B2-ZrCu (CsCl structure, Pearson symbol cP2, Space Group Pm $\bar{3}$ m, $a=0.3235$ nm), and the monoclinic martensitic B19'-ZrCu (P21/m space group, $a=0.3278$ nm, $b=0.4161$ nm, $c=0.5245$ nm, $\beta=103.88^\circ$). The alloy system is proved with good glass-forming ability.

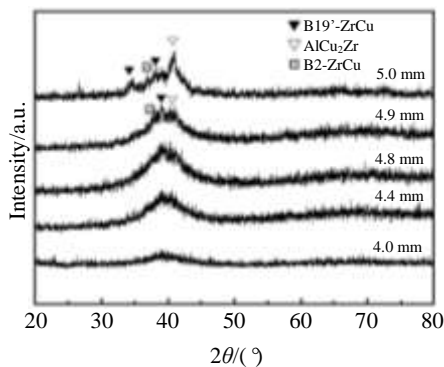


Fig.1 XRD patterns of tapered $\text{Cu}_{50}\text{Zr}_{42}\text{Al}_8$ samples with different diameters

Composites of crystals/amorphous structure in the sample of diameter 5.0 mm were observed in Fig.2. As the cooling rate changes, three different regions exist in the tapered sample, i. e. a surface amorphous region, a fine center equiaxial crystal region and a transition region between two regions. The crystal size and volume fraction increase from the surface to the center gradually.

Fig.3 shows different phases of BMG composites identified by TEM. We can see, amorphous matrix and three kinds of crystal structure are observed clearly from bright field image. The SAED pattern of the matrix shows a diffraction halo. Meanwhile, the brighter crystal phase “a” and adjacent darker crystal phase “b” are detected to be cubic AlCu_2Zr and ZrCu (pattern a and pattern b), respectively. Monoclinic martensitic ZrCu (pattern c), exists beside the B2-ZrCu, which is thermal-induced at the higher cooling rates of solidification in copper mould. Fig.4a and 4b shows the structure model of cubic AlCu_2Zr and ZrCu, respectively. The strongest covalent bond n_a of AlCu_2Zr is up to 0.4195, while n_a of B2-ZrCu with a weaker covalent is about 0.4093^[13]. As tangential motion of the packed plane needs to overcome a larger bonding force of atom pairs, far less plasticity is present in AlCu_2Zr .

2.2 Micro-mechanical properties of Cu based amorphous composites

Fig.5 shows Vickers micro-hardness of samples with diameter 4.0 and 5.0 mm along the radial direction. Compared

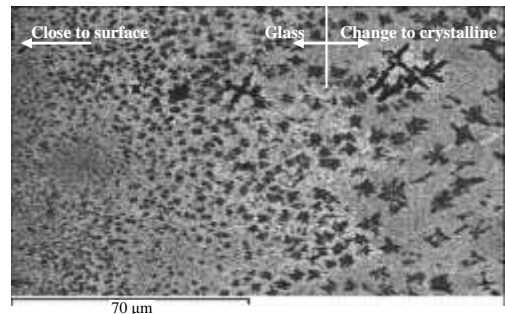


Fig.2 Metallographical structure of BMG composite of 5.0 mm in diameter

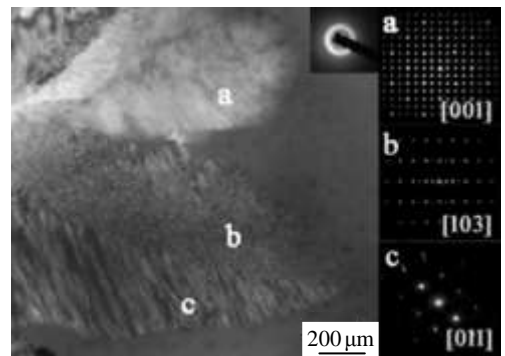


Fig.3 TEM Bright field image of BMG composites and SAED patterns from different regions (a-cubic AlCu_2Zr , b-cubic B2-ZrCu, c-monoclinic martensitic B19'-ZrCu)

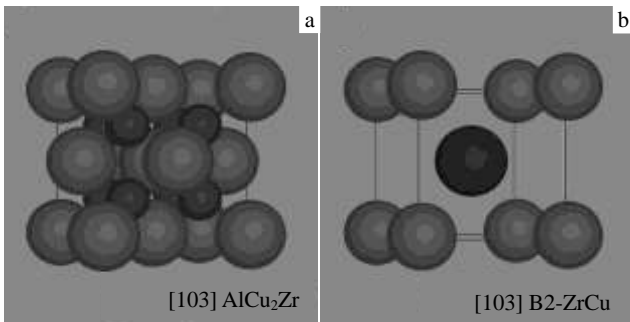


Fig.4 Structure model of cubic AlCu_2Zr (a) and ZrCu (b)

with the larger amorphous composites, monolithic BMG of 4.0 mm in diameter with close packing atomic structure displays significantly enhanced hardness as well as a "smaller is softer" trend. The phenomenon is attributed to the fact that the smaller size alloy, which experiences a faster cooling rate during solidification, contains a larger amount of heats of relaxation and free volume, thus forming a softer surface and a harder center^[14,15]. Whereas micro-hardness of larger size composites with a softer center and a harder surface, displays a "V" shape trend. As the microstructure evolves from disordered glass to order crystals, the hardness declines along with the increasing amount and growing crystals size.

The micro-mechanical properties and plastic deformation mechanism of 5.0 mm amorphous composites of different microstructure were studied by Nanoindenter, and the load-displacement curves of $\text{Cu}_{50}\text{Zr}_{42}\text{Al}_8$ BMG composites are shown in Fig.6. five points chosen from surface to center, points 1, 2 in amorphous area, 3, 4 in amorphous/crystal transition area, and point 5 in center crystal area, display obvious opposite trends of micro-hardness (H) and plastic deformation (d_n) (Fig.7). The surface amorphous structure is harder than the center crystal and the transition area. Point 2 is the hardest but the most brittle as the short-range ordered glass structure is lack of heats of relaxation and free volume during solidification. Whereas point 5 is the softest but weakest as the

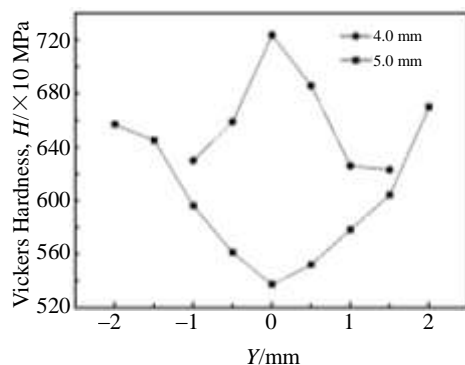


Fig.5 Vickers micro-hardness along the radial direction of the BMG composites with diameter of 4.0 and 5.0 mm

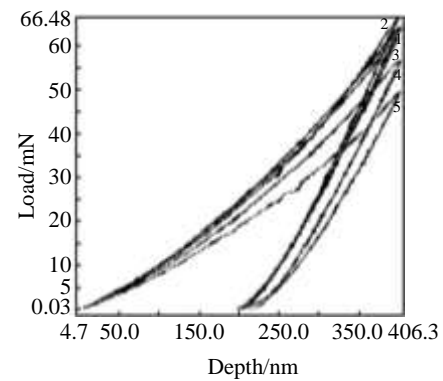


Fig.6 Nanoindentation load-displacement curves of $\text{Cu}_{50}\text{Zr}_{42}\text{Al}_8$ BMG composites at 1~5 points

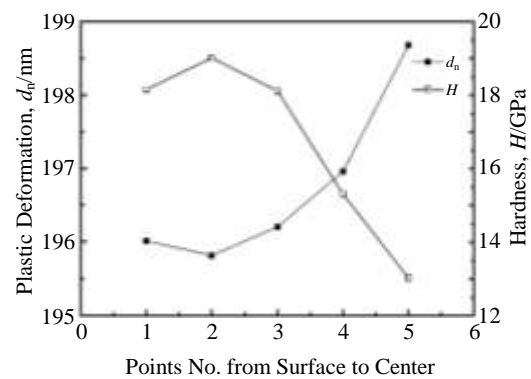


Fig.7 Micro-hardness and plastic deformation of 5 points at different regions of BMG composites

center crystal consists of cubic AlCu_2Zr , shape-memory B2-ZrCu and $\text{B19}'\text{-ZrCu}$. That is, the amorphous matrix is toughened by TRIP (Transition Induced Plasticity) effect of shape-memory phase as well as weakened and embrittled by AlCu_2Zr crystal. The micro-mechanical behavior depends on integrative action of the secondary phases.

2.3 Self-healing behavior of Cu based amorphous composites with shape-memory crystals

Self-healing behavior of Vickers indentation crack was observed when we tested the microhardness of tapered sample in the boundary of the glassy region and amorphous/crystal transition region. Initially cracks are evident in the cusp of diamond indentation towards boundary of the as-cast sample (Fig.8a). After annealed at 150 °C for 10 min, crack self-healing behavior and descending indentation area of the precracked specimen are obviously observed (Fig.8b). We conjecture that it is induced by phase transformation of the shape-memory crystals. The transformation is thermoelastic by observing the gradual growth and shrinkage of martensites upon cooling and heating, respectively^[16,17]. As loading, stress-induced martensites transformation occurs from B2 to B19', along with volume expansion owing to the larger volume of martensites than that of austenites. After annealed upon the reverse transformation temperature, B19' to B2

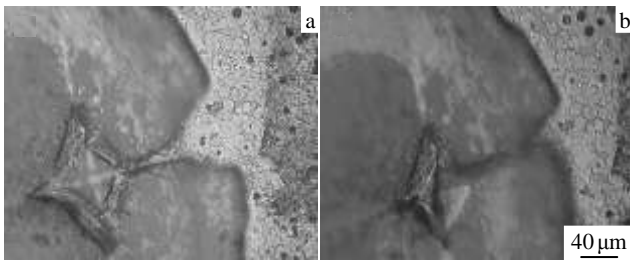


Fig.8 Vickers indentation crack: (a) metallograph of initially crack in as-cast specimen and (b) metallograph of the precracked specimen after annealed at 150 °C for 10 min

reverse transformation associated with a volume shrinkage occurs, and a restoring force from the structure stress is set up to drive the crack closure. Thus, we could achieve crack self-healing to monitor and control the structure.

3 Conclusions

1) $\text{Cu}_{50}\text{Zr}_{42}\text{Al}_8$ alloy has good glass-forming ability with maximum thickness up to 4.8 mm.

2) The complex structure of larger size consists of shape-memory B2-ZrCu, B19'-ZrCu and cubic AlCu_2Zr .

3) Compared with the larger amorphous composites (diameter >5 mm BMG), monolithic 4 mm BMG with close packing atomic structure displays significantly enhanced hardness as well as a "smaller is softer" trend. Whereas micro-hardness of the larger size composites with a softer center and harder surface, displays the opposite trend.

4) As loading by nanoindenter, martensites transition induced by plasticity occurs and toughens the amorphous matrix. Whereas the AlCu_2Zr crystal embrittles the composites, due to the larger covalent bond, that is, tangential

motion of packed plane needs to overcome a larger bonding force of atom pairs. After annealing, crack self-healing behavior and descending indentation area of the precracked specimen are obviously observed. That is attributed to phase transformation of the shape-memory crystals.

References

- 1 Wang W H. *Mater Prog Phys*[J], 2013, 33: 177
- 2 Pauly S, Liu G, Gorantla S et al. *Acta Mater*[J], 2010, 58: 4883
- 3 Zhang B, Zhao D Q, Pan M X et al. *Phys Rev Lett*[J], 2005, 94: 205 502
- 4 Liu Q, Kou S Z, Li C Y et al. *Rare Metal Materials and Engineering*[J], 2012, 41(11): 1891
- 5 Wang Y J, Suo Z Y, Qiu K Q et al. *Rare Metal Materials and Engineering*[J], 2012, 41(1): 96 (in Chinese)
- 6 Hofmann D C. *J Mater*[J], 2013, 2013: 517 904
- 7 Abbasi M, Gholamipour R, Shahri F. *Trans Nonferrous Met Soc China*[J], 2013, 23: 2037
- 8 Khademiana N, Gholamipour R. *J Non-Cryst Solids*[J] 2013, 365: 75
- 9 Wang Q, Qiang J B, Xia J H et al. *Intermetallics*[J], 2007, 15: 711
- 10 Wu J L, Pan Y, Li X Z et al. *Mater Des*[J], 2014, 57: 175
- 11 Das J, Tang M B, Kim K B et al. *Phys Rev Lett*[J] 2005, 94: 205501
- 12 Hofmann D C. *Science*[J], 2010, 329: 1294
- 13 Anthony L, Fultz B. *J Mater Res*[J], 1989, 4: 1132
- 14 Huang Y J, Shen J, Sun Y et al. *Mater Des*[J], 2010, 31: 1563
- 15 Huang Y J, Shen J, Sun J F. *Appl Phys Lett*[J], 2007, 90: 081 919
- 16 Otsuka K, Sawamura T, Shimizu K et al. *Phys Status Solidi*[J], 1971, 5: 457
- 17 Sandrock G D, Hehemann R F. *Metallography*[J], 1971, 4: 451

形状记忆晶相/铜基非晶复合材料的组织和微观力学行为

袁小鹏^{1,2}, 赵燕春^{1,2}, 寇生中^{1,2}, 赵志平^{1,2}, 李春燕^{1,2}, 袁子洲^{1,2}

(1. 兰州理工大学 省部共建有色金属先进加工与再利用国家重点实验室, 甘肃 兰州 730050)

(2. 兰州理工大学 温州泵阀工程研究院, 浙江 温州 325105)

摘要: 采用悬浮熔炼-水冷铜模吸铸法制备 $\text{Cu}_{50}\text{Zr}_{42}\text{Al}_8$ 锥形试样, 研究了合金不同直径处的组织和微观力学行为, 分析了尺寸效应和裂纹自愈合行为。结果表明, 复合材料组织中包含非晶基体相、金属间化合物 AlCu_2Zr 相、奥氏体 B2-ZrCu 相和热致马氏体 B19'-ZrCu 相。纳米压痕结果表明, 单一非晶结构的试样心部硬而表面较软, 呈现越小越软趋势, 而较大尺寸的非晶复合材料由于析出相的存在, 心部软而表面较硬。形状记忆晶相由 TRIP 效应对非晶基体增强增韧, 而 AlCu_2Zr 相析出使基体脆化。经 150 °C/10 min 退火后, 微观压痕产生的裂纹表现出自愈合行为。加载时, 形变诱导 B2 奥氏体向 B19' 马氏体相转变并伴随着体积的膨胀, 而高于逆转变温度退火, B19' 转变为 B2 相, 体积收缩并在组织应力作用下驱动裂纹愈合。

关键词: 非晶复合材料; 形状记忆晶相; 微观力学行为; 自愈合

作者简介: 袁小鹏, 1981 年生, 博士, 兰州理工大学省部共建有色金属先进加工与再利用国家重点实验室, 甘肃 兰州 730050, E-mail: 529782158@qq.com